Miniature Electrostatic, High-Vacuum Ion Pump Architecture Using A Nanostructured Field Emission Electron Source

A Basu[1] [a], **M A Perez**[b], **L F Velásquez-García**[2] [a]
a) Microsystems Technology Laboratories, Massachusetts Institute of Technology, 77 Massachusetts Avenue, Cambridge MA 02139, USA
b) ColdQuanta, Inc., 3030 Sterling Circle, Boulder, CO 80301, USA.

Abstract. We report a field emission-based, electrostatic ion pump architecture for generation of high vacuum within a small chamber that is compatible with miniaturized cold-atom interferometry systems. The design increases the ionization probability using a helical electron collector. To create vacuum, electrons from a nanostructured field emitter array impact-ionize the gas molecules within the chamber; then, the ions generated are gettered by a negatively charged annular-shaped titanium ion collector. A proof-of-concept pump prototype was developed and characterized using a 200 cm^3 stainless steel vacuum chamber. The pressure inside the chamber was observed to decrease from 7.8×10^{-7} Torr to 7.2×10^{-7} Torr as the bias voltage on the ion collector was varied from -100 V to -1000 V while the emission current was kept constant at approximately 3.2 μA. The functional form of the experimental pump characteristics is in agreement with a proposed reduced-order model.

1. Introduction

Cold-atom interferometry of alkali atoms can be harnessed to implement a variety of high-precision sensors and timing devices such as atomic clocks, gyroscopes, accelerometers, magnetometers and gravimeters [1]. These systems require ultra-high vacuum (UHV, pressure < 10^{-9} Torr) to operate; therefore, chip-scale atomic sensors and timing devices require miniaturized UHV pumps resilient to alkali metal vapours that consume power at levels compatible with device portability.

In a macro-sized chamber UHV-level vacuum can be maintained using a conventional magnetic ion pump, which consists of an array of positively charged cylinders (anode), a flat negatively charged Ti plate (ion collector), and large permanent magnets that generate high magnetic fields (~ 0.2 T) within the pump volume [2] to 'trap' the electrons and achieve efficient impact ionization. While scaled-down versions of magnetic ion pumps have been reported [3], these are incompatible with miniaturized cold-atom interferometry systems because (i) a reduction in the pump size causes the required threshold magnetic field for electron trapping to increase [4], and (ii) the larger magnetic field associated with a miniaturized ion pump can disrupt operation of the cold-atom interferometry systems [5]. Non-evaporable getter (NEG) pumps are used in some cold-atom interferometry systems, e.g., commercial chip-scale atomic clocks; however, NEG pumps are unable to pump noble gases such as He and N_2 that are present in the chamber, and they inefficiently pump alkali vapours.

In this work we report an improved magnet-free ion pump design compatible with chip-scale cold-atom interferometry devices. The pump design is shown to operate at orders of magnitude lower

[1] anirbasu@mit.edu
[2] Velasquez@alum.mit.edu

Content from this work may be used under the terms of the Creative Commons Attribution 3.0 licence. Any further distribution of this work must maintain attribution to the author(s) and the title of the work, journal citation and DOI.
Published under licence by IOP Publishing Ltd

pressure compared to the pump described in [6]. In addition, the pump speed, characterized by the pumping time constant τ, is shown to be much larger than the pump speed of our previous pump design reported in [7], which also was implemented in a 200 cm^3 chamber.

2. Device Design

The proposed field emitter array (FEA)-based magnet-free ion pump architecture is shown in Figure 1. In this pump design, a helical electron collector pulls the electrons toward itself, forcing them to first travel beyond the height of the electron collector, to then get pushed back due to the electrostatic mirror effect of the annular-shaped ion collector. Therefore, the trajectory of the electrons is significantly increased compared to a pump design with parallel-capacitor electrode configuration, such as the one described in [8], augmenting the probability of impact ionization.

Figure 2 shows a picture of the implemented proof-of-concept pump prototype assembled on a 2.75" CF flange with four electrical feedthroughs. The FEA chip is placed on top of a glass substrate. Two spring clips, one for the chip substrate and the other for the gate electrode pad, are used to provide mechanical stability as well as electrical connection between the chip and the feedthroughs. The two other electrical feedthroughs of the flange were connected to the ion and electron collectors via copper wires. The ion collector is made of titanium to efficiently getter ions, while the electron collector is made of a refractory metal to facilitate being heated to high temperatures when a current is passed through it during baking of the apparatus, thus reducing the outgassing of the electrode when the pump is in operation. The chamber is connected through an all-metal valve to an external support pump system that is not shown in the picture.

The FEA (Figure 3) consists of 62,500 nano-sharp silicon tips, each surrounded by a self-aligned gate electrode; the fabrication of the FEA is described elsewhere [9]. The nanometer-sharp tips generate high surface electric fields (>3×10^7 V/cm) at low bias voltage (< 40 V), causing electrons to quantum-tunnel to vacuum [10]. In a previous publication we showed that these FEAs do not degrade in the presence of Rb vapour [7].

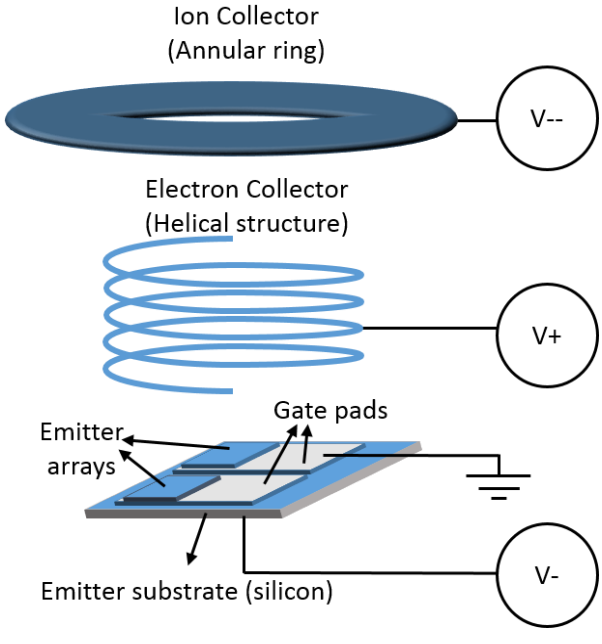

Figure 1. Schematic of the FEA-based, magnetic-less ion pump architecture.

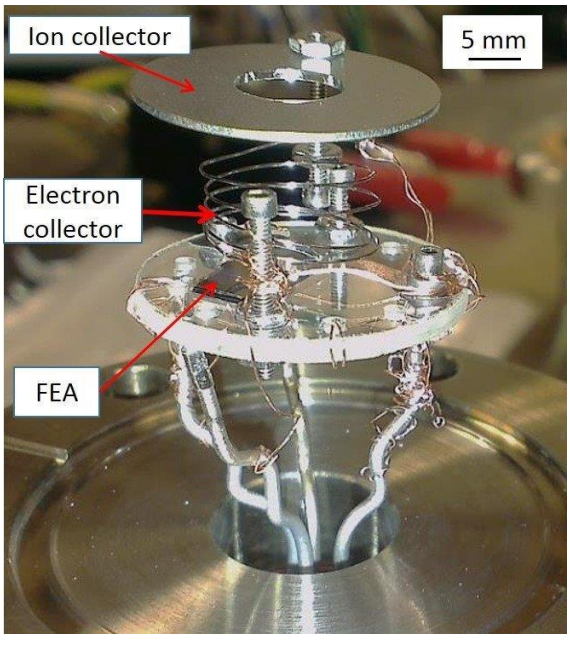

Figure 2. Picture of the FEA-based ion pump showing the electron and ion collectors.

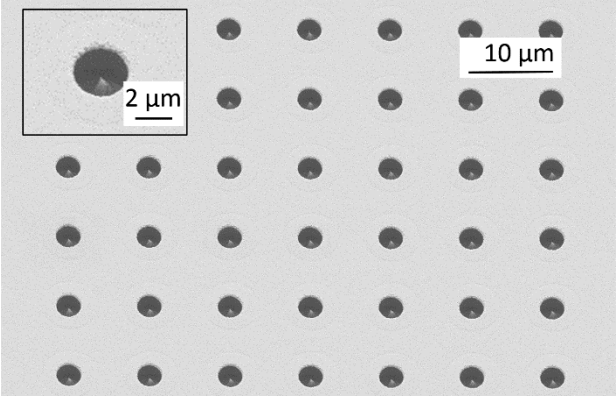

Figure 3. SEM of a section of the active area of the FEA chip, showing the nano-sharp tips surrounded by gate electrode apertures.

3. Device Modelling

Finite-element simulations using the commercial software COMSOL Multiphysics were conducted on a 3-D model of the proof-of-concept pump prototype. The helical electron collector has an outer diameter of 1.5 cm and a wire thickness of 0.4 mm; the ion collector is an annular structure with 2.5 cm outer diameter and 0.8 cm inner diameter, while the active area of the field emission electron source is a square 4 mm wide. The initial kinetic energy of the electrons was assumed to be 100 eV, which corresponds to a bias voltage between the chip substrate and the gate electrode equal to 100 V. Figure 4 shows the trajectories of 100 electrons evenly spread across the top surface of the electron source. In this simulation, the ion collector was biased at -1000 V, while the electron collector was biased at +1000 V. The simulation results show that the trajectory of the electrons is significantly increased compared to the parallel capacitor case, which results in an increased ionization probability.

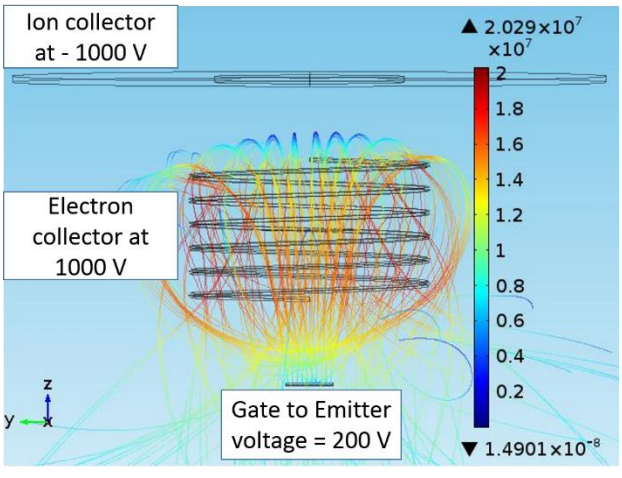

Figure 4. Finite element analysis of the trajectories of the electrons emitted by the FEA in the proposed ion pump design. The scale bar shows the speed of the electrons in m/s.

The theoretical relationship between chamber pressure as a function of time, volume of the chamber, and emitted electron current can be derived from first principles starting from the ideal gas law; the ion current is given by the electron impact ionization model. It can be shown that the chamber pressure P as a function of time t is equal to

$$P(t) = [P_o - P_f]e^{-t/\tau} + P_f \quad (1)$$

where P_o is the chamber pressure at $t = 0$, P_f is the ultimate pressure of the chamber ($t \gg \tau$), and τ is the characteristic pumping time constant, which is a function of chamber volume, electron current, length of the trajectory of the electrons, and ionization cross section of the gas species. Given the functional dependence of the chamber pressure versus time predicted by (1), the semi-log plot of the negative of the time derivative of the pressure versus time describes a straight line with slope equal to -1/τ, i.e.,

$$ln\left[-\frac{dP(t)}{dt}\right] = ln\left[\frac{P_o - P_f}{\tau}\right] - \frac{t}{\tau} \quad (2)$$

4. Experimental Results

4.1 FEA Characterization

The FEA chip was characterized in a UHV chamber maintained at 5×10^{-10} Torr pressure. The current versus voltage (*I-V*) characteristics of the device are shown in Figure 5; the electron source turns-on with 32 V of bias voltage and emits over 1 mA with 99.8% transmission through the gate when biased at 117 V. Figure 6 shows the Fowler-Nordheim (*F-N*) plot of the data shown in Figure 5, i.e., $ln\ (I/V^2)$ vs. $1/V$ where I is the transmitted (collected) current and V is the bias voltage; the data describe a straight line, demonstrating that the current is field emitted. Using modelling reported in [9], from the slope of the F-N plot the radius of the tips is estimated at 1.73 nm, in agreement with SEM metrology.

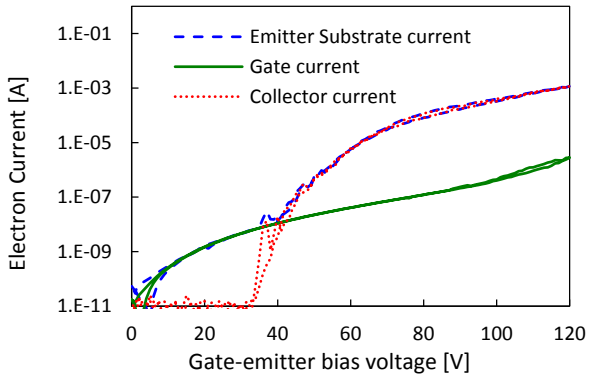

Figure 5. Current-voltage characteristics of the silicon FEA. The current is dominated by gate leakage until ~40 V, after which is mostly transmitted by the gate electrode.

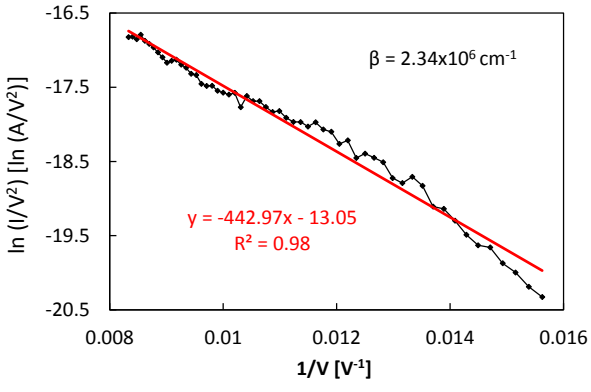

Figure 6. Fowler-Nordheim plot of the collected electron current from the FEA chip. A field factor β equal to 2.34×10^6 cm^{-1} is obtained from the slope of the plot.

4.2 Pump Characterization

Figure 7 shows the pressure versus time data collected with the proof-of-concept pump prototype. The data were acquired starting at the point when pressure is at 7.3×10^{-7} Torr and the ion collector was biased at -1000 V. The chamber pressure rises to 7.8×10^{-7} Torr when the bias voltage on the ion collector is set to -100 V, and it is seen to fall when the voltage is set to -1000 V with the lowest observed pressure being 7.2×10^{-7} Torr. Throughout the test, there was no variation in the emission current observed, showing that pumping was due to the ion collector voltage alone and not due to other factors such as reduced electron scrubbing as observed in [7]. Figure 8 shows the semi-log plot of the minus time derivative of the pressure versus time during pump-down, with the horizontal axis denoting the time since the beginning of each pump-down cycle. Each data point in the plot represents an average of the minus time derivative of the pressure considering all pump-down cycles. The slope of the linear fit of the data estimates the experimental pumping time constant at about 161 seconds.

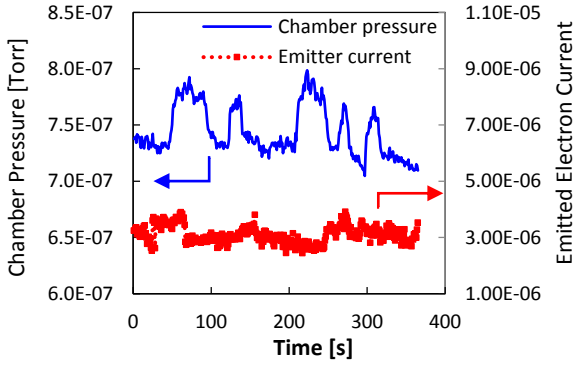

Figure 7. Pressure versus time. Pressure falls when the ion collector is biased at -1000 V, and it rises when the voltage is set to -100 V.

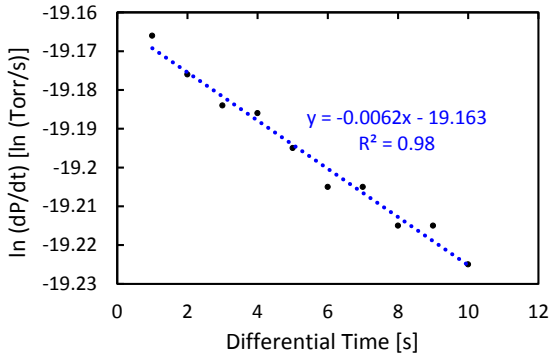

Figure 8. Semi-log plot of the negative of the time derivative of the chamber pressure vs. time. From the slope of the linear fit $\tau = 161.2$ s.

5. Conclusion

An improved proof-of-concept magnet-free pump prototype was implemented in a 200 cm^3 stainless steel vacuum chamber. The architecture consisted of a silicon FEA chip as electron source, a helical electron collector made of a refractory metal, and an annular ion collector made of titanium. Characterization of the FEA chip demonstrates that the electrons produced are field emitted. Characterization of the ion pump prototype shows that the pressure inside the chamber rapidly decreases from 7.8×10^{-7} Torr to 7.2×10^{-7} Torr as the bias voltage on the ion collector is varied from -100 V to -1000 V at a constant electron current of 3.2 μA, achieving a vacuum level that is orders of magnitude below the best reported values from a miniaturized magnetic-free ion vacuum pump. A reduced-order model of the pump dynamics predicts the functional form of the pumping data.

Acknowledgments

The fabrication of the nanostructured field emission electron source was done by Arash Fomani from MIT and was carried out in the Microsystems Technology Laboratories, MIT. We would like to thank Steve Hughes from ColdQuanta and David Johnson from Draper Laboratories for helpful discussions. This work was funded by the Defence Advanced Research Projects Agency / Microsystems Technology Office (DARPA/MTO) award number 022995-001 (program manager Robert Lutwak). Any opinions, findings, and conclusions or recommendations expressed in this publication are those of the authors and do not necessarily reflect the views of the US Government and therefore, no official endorsement of the US Government should be inferred.

6. References

[1] Kitching J, Knappe S, and Donley E A 2011 *IEEE Sensors Journal* **11** 1749
[2] Welch K 2001 *Capture pumping technology* (Elsevier)
[3] Green S R, Malhotra R, and Gianchandani Y B 2013 *J. Microelectromech. Syst.* **22** 309
[4] Audi M and De Simon M 1987 Vacuum **37** 629
[5] Rushton J A, Aldous M, and Himsworth M D 2014 *e-print arXiv:1405.3148*
[6] Grzebyk T, and Górecka-Drzazga A 2013 *J. Micromech. Microeng.* **23** 015007
[7] Basu A, Perez M A, Velasquez-Garcia L F 2015 *Proc. 18th Int. Conf. on Solid-State Sensors, Actuators and Microsystems* (Anchorage, AK) pp1021-1024
[8] Fomani A A, Velásquez-García L F, and Akinwande A I 2014 *Proc. 27th Int. Vacuum Nanoelectronics Conference* (Engelberg, Switzerland) pp. 210-211.
[9] Basu A, Swanwick M E, Fomani A A, and Velásquez-García L F 2015 *J. Phys. D: Appl. Phys.* **48** 25501
[10] Gomer R 1961 *Field emission and field ionization* (Cambridge, MA: Harvard University Press)